Theor Chem Acc (2011) 128:619–626
DOI 10.1007/s00214-010-0826-3

REGULAR ARTICLE

On the mechanism of the *N*-glycosydic bond hydrolysis of 2′-deoxyguanosine: insights from first principles calculations

R. Rios-Font · J. Bertran · M. Sodupe · L. Rodríguez-Santiago

Received: 21 June 2010 / Accepted: 14 September 2010 / Published online: 30 September 2010

Abstract The effect of the activation of the nucleobase (leaving group) or the activation of the water molecule (nucleophile) by a general acid or a general base on the hydrolysis of the *N*-glycosydic bond of 2′-deoxyguanosine has been analyzed by means of density functional methods. First, we have considered two limiting cases: (1) the activation of the guanine by protonation at N7 and (2) the nucleophile attack by a hydroxyl ion, to separately evaluate the two kinds of activation. Next, we have studied the simultaneous activation of the leaving group and the nucleophile by introducing models of amino acid residues such as a formic acid (HCOOH) and imidazolium ($C_3N_2H_5^+$), methylammonium ($CH_3NH_3^+$) and formate ($HCOO^-$) ions in the system. It is shown that protonation of the nucleobase greatly catalyzes the hydrolysis of the *N*-glycosydic bond, the reaction occurring through a stepwise (D_N*A_N) mechanism with a discrete oxocarbenium ion intermediate. However, when a H_2O nucleophile molecule is activated by a formate anion, the reaction mechanism is a concerted A_ND_N but with different degrees of dissociative character of the transition structure depending on the acid that is activating the nucleobase.

Keywords *N*-glycosydic bond hydrolysis · 2′-Deoxyguanosine · DNA repair mechanisms · DFT · Leaving group activation · Nucleophile activation

Published as part of the special issue celebrating theoretical and computational chemistry in Spain.

R. Rios-Font · J. Bertran · M. Sodupe · L. Rodríguez-Santiago (✉)
Departament de Química,
Universitat Autònoma de Barcelona,
08193 Bellaterra, Spain
e-mail: Luis.Rodriguez.Santiago@uab.cat

1 Introduction

The stability of the *N*-glycosydic bond between the deoxyribose sugar and a nucleobase is extremely important to maintain the integrity of the hereditary material stored in DNA. On the one hand, the hydrolysis of the *N*-glycosydic bond, which may occur spontaneously or induced by chemical damage, leads to the formation of apurinic/apyrimidinic sites that may be potential sources of mutagenesis [1]. On the other hand, the removal of damaged nucleobases from DNA, first by base flipping [2–4] and second by bond cleavage of the *N*-glycosydic bond, is the first process in the enzymatic base excision repair (BER) mechanism of DNA [5–7]. This nucleobase removal is carried out by DNA glycosylases, which are classified as monofunctional or bifunctional [5, 6]. The former ones use a water molecule to attack the anomeric carbon of the damaged nucleotide and hydrolyze the glycosydic bond, whereas bifunctional enzymes remove the nucleobase by glycosyl transfer using an amine nucleophile of the enzyme.

Due to the importance of the *N*-glycosydic bond, many studies have been devoted to understand the mechanism by which the glycosydic bond is hydrolyzed (see references [5] and [6] and references therein). These include enzymatic structural and inhibition studies, kinetic isotope effect (KIE) analysis of DNA glycosylases or related systems and non-enzymatic studies of the pH dependence of the hydrolysis. These studies have shown that the enzymatic cleavage mechanism of the *N*-glycosydic bond is different for purine and pyrimidine nucleobases [5, 6, 8]. In the case of purines, protonation of the nucleobase to make it a better leaving group catalyzes the hydrolytic cleavage [8–10]. Another generally invoked factor is the activation of the nucleophile by a close base [8, 11–14]. The amino

acid residues directly involved in the protonation of the nucleobase and the nucleophile activation are not well identified, and the proposed mechanisms use a general acid and a general base as catalysts [5, 6, 15].

The hydrolysis of the *N*-glycosydic bond can proceed either through a concerted S_N2 reaction or through a stepwise S_N1 mechanism [5, 6]. The S_N2 reaction is referred as A_ND_N to indicate that there is a nucleophile addition (A_N) and a nucleophile dissociation (D_N) in the transition structure. Furthermore, this A_ND_N mechanism is designated as associative or dissociative depending on whether there is a significant bond order between the sugar and the attacking nucleophile and leaving group in the transition structure. The stepwise mechanism is termed $D_N{*}A_N$ or $D_N + A_N$ to indicate that the leaving group departure precedes the nucleophile addition, the difference between the two mechanisms being the lifetime of the oxocarbenium ion intermediate: short-lived in $D_N{*}A_N$ and fully solvent equilibrated in $D_N + A_N$. Transition state analyses have revealed that the mechanism of glycosyde hydrolysis lies within the borderline between a stepwise $D_N{*}A_N$ (S_N1) and a highly dissociative A_ND_N (S_N2) mechanism [8, 16–18].

The knowledge of how different factors influence the mechanism of this reaction is important to understand how DNA glycosylases function. In this context, quantum chemical calculations can provide useful information to understand the relative contributions of leaving group and nucleophile activation. Indeed, several studies have used computational chemistry to get specific information at a molecular level on pyrimidine [11, 19–25] and purine deoxynucleosides [24–35]. However, few previous quantum chemical studies have considered the hydrolysis mechanism of 2′-deoxyguanosine (dG) [24, 25, 33, 35]. Both neutral [24, 25, 33, 35] and N7-protonated [33] dG have been considered, showing that nucleobase protonation plays a fundamental role in the catalysis of this reaction. Moreover, Wetmore et al. [24, 35] have considered different nucleophile molecules including activated water. The present work extends our previous study and systematically analyzes how either the activation of the leaving group or the activation of the nucleophile by a general acid or a general base influences the mechanism of the reaction. In particular, we study the simultaneous activation of the leaving group and the nucleophile by introducing models of amino acid residues such as a formic acid (HCOOH) and imidazolium ($C_3N_2H_5^+$), methylammonium ($CH_3NH_3^+$) and formate ($HCOO^-$) ions in the system. While these are reduced model systems, their size allows us to perform quantum chemical calculations at a reasonable level of theory and get insights of the acid–base catalysis in this kind of systems.

2 Computational details

Full-geometry optimizations and harmonic vibrational frequency calculations for all different species under consideration have been performed using the non-local three-parameter hybrid exchange B3LYP [36, 37] density-functional method with the 6-31++G(d,p) basis set. However, the hydrolytic cleavage of the *N*-glycosydic bond is a nucleophilic substitution, which may be either a S_N2 or a stepwise S_N1 reaction, and S_N2 reactions have been shown to be quite sensitive to the amount of exact exchange included in the functional. Benchmark calculations carried out in our previous study [33] on the hydrolysis of 9-methylguanine using the B3LYP (20% exact exchange), the MPWB1K [38] (44%) and the BHandHLYP [37, 39] (50%) density-functional methods have shown that the optimized structures of reactants, products and transition structures obtained with the three functionals are basically identical, the largest difference (0.09 Å) corresponding to the N9-C distance in the transition structure TS. Moreover, because for the hydrolysis of 9-methylguanine, the energy profile computed with B3LYP was found to be in reasonable good agreement with the one obtained from CCSD(T) [40] single-point calculations at the B3LYP optimized geometries, results for all the remaining systems were performed at the B3LYP level. In all cases, intrinsic reaction coordinate (IRC) calculations were carried out in order to identify the minima connected by a given transition structure.

All calculations were performed with the GAUSSIAN 03 program package [41]. Thermochemical corrections to the energy values were computed using the standard rigid rotor/harmonic oscillator formulae [42]. Solvent effects were introduced using the conductor polarized continuum model (CPCM) [43], at the gas-phase optimized geometries. This is the strategy generally used in similar systems [24, 35] and is not expected to modify the major conclusions of the work. Finally, to analyze the stereoelectronic effects, natural bond orbital (NBO) analysis of Weinhold and Carpenter was carried out [44, 45]. It should be mentioned that all calculations have been performed using a slightly modified 2′-deoxyguanosine (see Scheme 1), in which the hydroxyl group of C3′ has been substituted by OCH_3, to avoid spurious hydrogen bonds with the incoming H_2O molecule.

3 Results

As mentioned, in this paper we analyze how the activation of the leaving group or the activation of the nucleophile influences the mechanism of the *N*-glycosydic bond hydrolysis of 2′-deoxyguanosine (dG). Thus, results will be organized as follows. First, we will present the results for

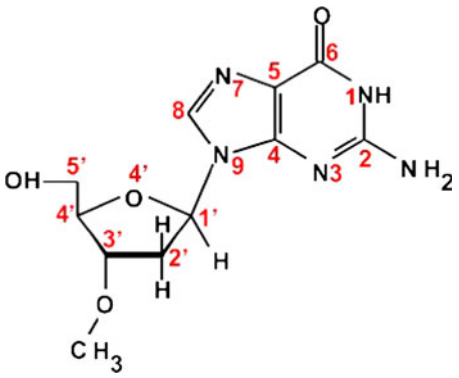

Scheme 1 Numbering of the most relevant centers of 2′-deoxyguanosine

N7 guanine-protonated systems (**HdG**). Second, we will consider the nucleophilic attack of OH^- on dG (**dG + OH^-**). These two situations represent the two limiting cases associated with the activation of the leaving group and of the H_2O nucleophile, respectively, and will allow us to separately evaluate the two kinds of activation and how they contribute to the mechanism of the reaction. Next, we will consider the simultaneous activation of the leaving group and the nucleophile.

3.1 Leaving group activation. Mechanism of N7-protonated 2′-deoxyguanosine (HdG) + H_2O

Purines are susceptible to acid catalysis by N-protonation because this helps to accommodate the increased electron density that is developed during the glycosydic bond cleavage. Since N7 is the most basic site in dG, we have considered protonation to take place at this site. Figure 1 shows the potential energy profile and the optimized structures of the relevant species involved in the mechanism. It can be observed that the hydrolysis of the N–C bond occurs through a stepwise mechanism. The first step is the formation of an oxocarbenium-like intermediate (**I1**) through a transition structure (**TS1**) that presents a C1′–N9 bond distance of 2.33 Å. This value is very similar to that previously reported [33] (2.32 Å), although the orientation of the water molecule in the transition structure is now somewhat different. In the present work, H_2O establishes a hydrogen bond with the O bound to the C3′ of 2′-deoxyribose, whereas in our previous study, H_2O establishes a hydrogen bond with the N3 of guanine. Nevertheless, this change in orientation of the attacking H_2O molecule produces a small variation ($\sim$1.5 kcal mol^{-1}) on the activation energy of the reaction. In the present case, $\Delta G^{\ddagger}$ with respect to the reactant $H^+dG_{N7}\cdots H_2O$ complex is 15.7 kcal mol^{-1} (17.6 kcal mol^{-1} if referred to the $H^+dG_{N7} + H_2O$ asymptote), whereas in our previous study, the $\Delta G^{\ddagger}$ value, reported with respect to the $H^+dG_{N7} + H_2O$ asymptote, was found to be 19.1 kcal mol^{-1}. The **I1** intermediate, obtained from IRC calculations, is only 0.5 kcal mol^{-1} (0.9 kcal mol^{-1} in terms of Gibbs energy) below **TS1** and shows a C1′–N9 distance that is significantly larger than in **TS1** (2.80 vs. 2.33 Å). Changes in the $O_{nucl}\cdots C1'$ distance are much smaller, the computed values being 2.78 Å in **TS1** and 2.50 Å in **I1**. In addition to **I1**, another more stable

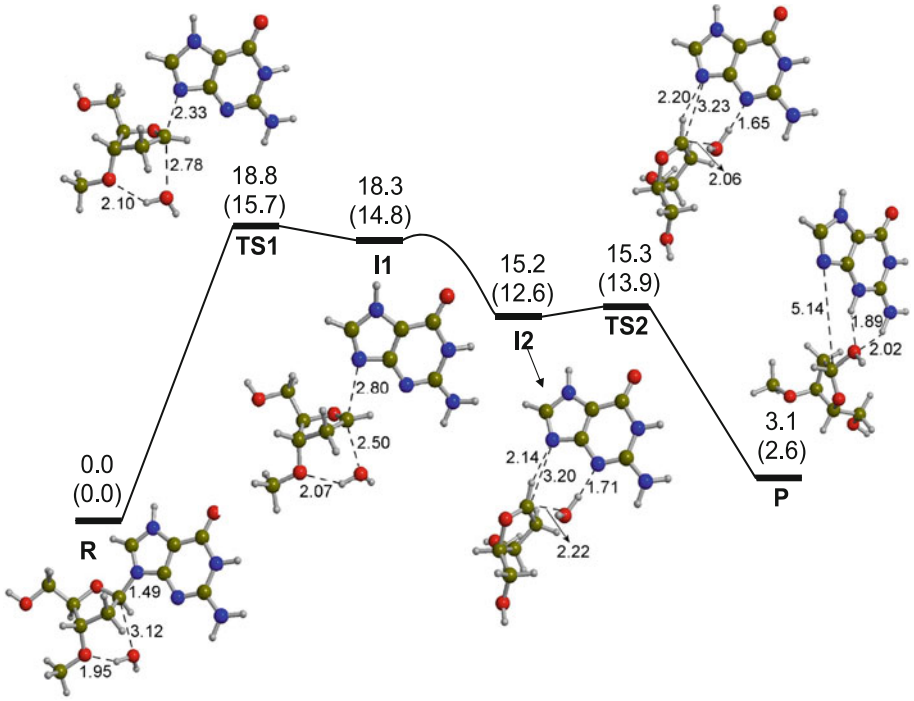

Fig. 1 Potential energy profile (Gibbs energies in *parenthesis*) for the hydrolysis of N7-protonated 2′-deoxyguanosine (**HdG**) and optimized geometries of the involved species. Bond distances are in Å and energies in kcal mol^{-1}

oxocarbenium-like intermediate (**I2**), in which a hydrogen bond interaction between the positively charged oxocarbenium and N9 of guanine occurs, has also been located. Attempts to localize the transition structure connecting both intermediates failed because the potential energy hypersurface is very shallow in this region. In this intermediate, the attacking water molecule establishes an additional H-bond with N3 of guanine, which allows a more efficient interaction with the sugar that manifests in a significantly shorter $O_{nucl}\cdots C1'$ distance (2.22 Å). From this intermediate, the nucleophilic attack of water to the C1′ atom of the oxocarbenium ion occurs very easily, since the Gibbs free energy barrier is only 1.3 kcal mol^{-1}. Note that this reaction leads to a tautomer in which N9 is deprotonated and N3 and N7 are protonated. Overall, these results indicate that the *N*-glycosydic bond hydrolysis of N7-protonated 2′-deoxyguanosine occurs easily through a stepwise (D_N*A_N) mechanism with a discrete oxocarbenium ion intermediate. Protonation of the guanine at N7 has an important catalytic effect, i.e., the computed energy barrier is much smaller than that of the neutral system [25, 33], since it helps to accommodate the negative charge that is generated in the nucleobase during the hydrolysis.

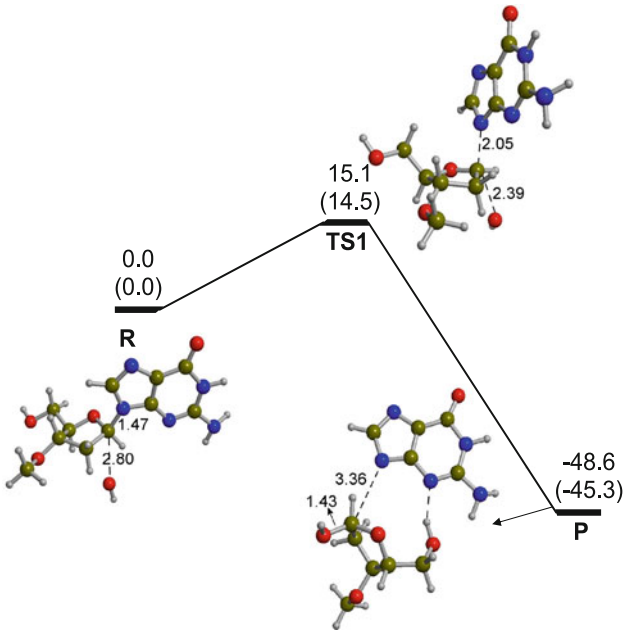

Fig. 2 Potential energy profile (Gibbs energies in *parenthesis*) for the nucleophile attack of OH^- to 2′-deoxyguanosine and optimized geometries of the involved species. Bond distances are in Å and energies in kcal mol^{-1}

3.2 Nucleophile activation. Mechanism of 2′-deoxyguanosine (dG) + OH^-

As previously mentioned, activation of the water molecule by a base has been invoked to be an important factor in the catalytic hydrolysis of the *N*-glycosydic bond [6]. In order to analyze the role of nucleophile activation, we have first considered the limiting case in which the water molecule is deprotonated by a nearby base and so the nucleophile attack is carried out by a hydroxyl ion. The potential energy profile and the optimized structures of the relevant species involved in the process are shown in Fig. 2. It can be observed that the $O_{nucl}\cdots C1'$ distance in the reactant (2.80 Å) is much shorter than that in the previous case (3.12 Å) and that the reaction takes place through a concerted mechanism with a more compact transition structure. Both the C1′–N9 and the $O_{nucl}\cdots C1'$ distances in the transition structure are shorter than those in the protonated case (2.05 vs. 2.33 Å and 2.39 vs. 2.78 Å, respectively), the energy barrier (either potential or Gibbs energy) being somewhat smaller for the OH^- attack (see Figs. 1, 2) and similar to the values previously reported [24, 35]. Thus, nucleophile activation has also an important catalytic effect on the hydrolysis reaction. The major difference between both situations (leaving group vs. nucleophile activation) appears in the mechanism; i.e., while the activation of the leaving group by protonation leads to a stepwise (D_N*A_N) mechanism with a discrete oxocarbenium ion intermediate, the hydrolysis reaction using a strong nucleophile such as the hydroxyl anion leads to a concerted A_ND_N mechanism. Since both strategies have been suggested for enzymatic processes, the mechanism of the hydrolysis of 2′-deoxyguanosine when the leaving group and the nucleophile are simultaneously activated may be S_N1 or S_N2 as it will be analyzed in the next section.

3.3 Simultaneous leaving group and nucleophile activation

Different amino acid residues such as aspartic or glutamic acids and protonated histidine, lysine or arginine have been invoked to activate the leaving group. In the case of the nucleophile activation, glutamate has been proposed as responsible for the deprotonation of the attacking water molecule [8]. Thus, for the activation of the water molecule, we considered a formate ion ($HCOO^-$), and for the activation of the leaving group, we considered, as models of the previously mentioned amino acids, a formic acid (HCOOH), an imidazolium ($C_3N_2H_5^+$) and a methylammonium ($CH_3NH_3^+$) molecule. In addition, we also considered the case in which guanine is just protonated. For the sake of brevity, the studied systems will be designated as **XdGY** where **X** indicates the group activating the nucleobase (**H** for the proton, **Fmc** for the formic acid, **ImH** for the protonated imidazole and **NH** for the protonated methylamine) and **Y** indicates the activating water group, which is always a formate anion (**Fmt**).

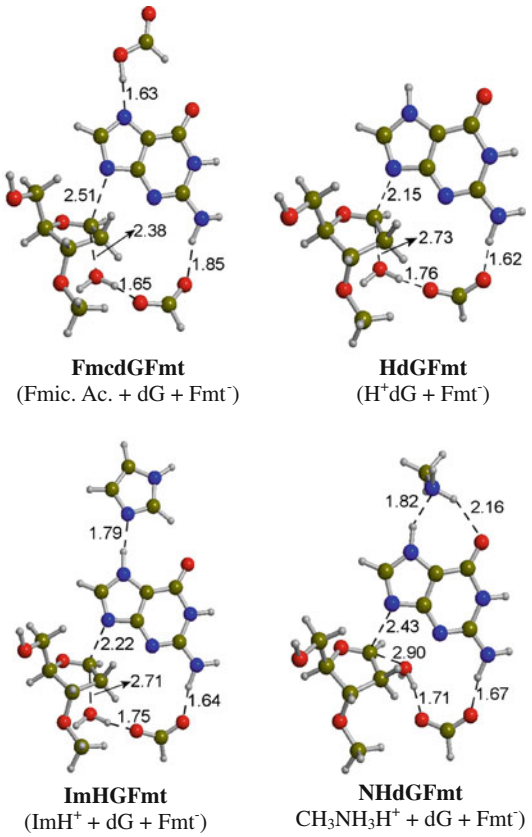

Fig. 3 Transition structures optimized geometries of the hydrolysis of N7-protonated 2′-deoxyguanosine with simultaneous activation of the leaving group and the nucleophile. Bond distances are in Å

Table 1 Total charge of the system, mechanism, reaction energies, barrier energies and activation solvation free energies of the studied reactions

System	Q_{total}	Mech.	$\Delta E^{\ddagger}$	$\Delta G^{\ddagger}$	$\Delta\Delta G^{\ddagger}_{solv}$	ΔE	ΔG
HdG	+1	$D_N{*}A_N$	18.9	15.7	4.1	–	–
dGOH	−1	A_ND_N	15.1	14.5	7.2	−48.6	−45.3
FmcdGFmt	−1	A_ND_N	33.0	31.7	−4.2	−3.0	−2.3
HdGFmt	0	A_ND_N	18.8	17.7	3.0	−20.0	−21.1
ImHdGFmt	0	A_ND_N	21.2	20.1	0.2	−15.3	−16.1
NHdGFmt	0	A_ND_N	20.3	17.6	2.4	−16.0	−16.9

Energies are in kcal mol^{-1}

Figure 3 and Table 1 show the optimized geometries of the transition structures of the considered reactions as well as the reaction energies, the energy barriers, the total charge of each system, the mechanism of the reactions and the activation solvation free energies. As presented in Table 1, in all cases where both the leaving group and the nucleophile are activated, the reaction takes place through a concerted A_ND_N mechanism. However, there are meaningful differences between the different considered systems. Figure 3 shows that in all the transition structures, the formate group forms two hydrogen bonds, one with the water molecule and the second one with the NH_2 group of the guanine nucleobase. It should be noted that the water molecule is not yet deprotonated in the transition structure.

If we compare the structures of Fig. 3, it appears that in the case of the system activated by a formic acid molecule and a formate anion (**FmcdGFmt**), the C1′–N9 distance is the largest one (2.51 Å) while the $O_{nucl}\cdots C1'$ is the shortest one (2.38 Å), thus indicating that this is the most dissociative process. In this case, the formic acid establishes a strong hydrogen bond with the N7 atom of guanine, being the only situation where the guanine is not protonated. In all of the remaining systems, **HdGFmt**, **ImHdGFmt** and **NHdGFmt**, the nucleobase is protonated at the N7 position. In these three cases, the C1′–N9 distance is shorter than in **FmcdGFmt** and the $O_{nucl}\cdots C1'$ distance is larger. It should be mentioned that in **HdGFmt** and **ImHdGFmt**, the C1′–N9 distance (2.15 and 2.22 Å) is even shorter than in the limiting case where only the leaving group was activated, **HdG** (2.33 Å, see Fig. 1), indicating the effect of the water activation by the formate anion. Particularly interesting is the comparison between **ImHdGFmt** and **NHdGFmt**, where both the C1′–N9 and $O_{nucl}\cdots C1'$ distances are much larger for the latter transition structure than for the former one. This may be related to the fact that the methylamine group, in addition to acting as a proton acceptor with the protonated N7 site, it also acts as a proton donor in a hydrogen bond with the O6 atom of guanine.

Table 1 shows that the computed activation energies follow the Hammond principle since in all four cases, the activation barrier decreases as the stability of the product increases. It can also be observed that the activation of the leaving group by formic acid (**FmcdGFmt**) is significantly less efficient than that in the other systems where the N7 position is protonated. Note that the energy barrier for **FmcdGFmt** is 33.0 kcal mol^{-1}, whereas for the protonated systems (**HdGFmt**, **ImHdGFmt** and **NHdGFmt**), the computed values are much smaller (18.8–21.2 kcal mol^{-1}). Remarkably, the potential energy barrier for **HdGFmt** (18.8 kcal mol^{-1}) is almost identical to the case where only the leaving group is activated, **HdG,** (18.9 kcal mol^{-1}) in spite of the significant differences found in the geometries (see above). For **ImHdGFmt** and **NHdGFmt**, potential energy barriers are slightly larger (21.2 and 20.3 kcal mol^{-1}, respectively) than those for **HdGFmt**, in agreement with the fact that in these cases protonated guanine establishes a hydrogen bond with the imidazole and methylamine groups, reducing the positive charge at the guanine moiety. The differences observed in the values of the C1′–N9 and $O_{nucl}\cdots C1'$ distances in the two systems are, however, quite remarkable since they are about 0.2 Å larger in **NHdGFmt** than in **ImHdGFmt**, the potential energy barrier being somewhat lower in

NHdGFmt. This may be due to the different hydrogen bond interactions established with the leaving group in the two systems. Note that in **NHdGFmt**, O6 forms a hydrogen bond with methylamine, which may induce electronic changes at the guanine moiety.

3.4 General trends

The comparison of the energetic parameters of all the studied systems, shown in Table 1, will allow us to rationalize the different factors implied in the catalytic process. It can be observed in Table 1 that when only the leaving group is activated (**HdG**), the reaction takes place through a D_N*A_N mechanism. However, in all the remaining cases, the reaction corresponds to an A_ND_N mechanism. In particular, although the potential energy barrier for the **HdG** and **HdGFmt** systems is almost identical, the mechanism changes substantially, thus indicating that nucleophile activation has little influence on the barrier but an important role in the mechanism.

If we compare the values for the potential energy and free energy barriers, it can be noted that the latter ones are always smaller. Thus, the entropic term ($\Delta S^{\ddagger}$) of the process is favorable, showing that in all cases, the transition structure is more flexible than the reactants, in agreement with a dissociative mechanism. Focusing on the two limiting cases, it can be observed that the difference between $\mathbf{\Delta E^{\ddagger}}$ and $\mathbf{\Delta G^{\ddagger}}$ is the largest one for **HdG** (3.2 kcal mol^{-1}) and the smallest one for **dGOH** (0.6 kcal mol^{-1}), in agreement with the fact that **HdG** shows a D_N*A_N mechanism, while **dGOH** shows the less dissociative transition structure. Moreover, the decrease in the activation free energy is also important for **NHdGFmt**, with a less compact transition structure when compared to the other systems with a simultaneous activation of the leaving group and the nucleophile. Consequently, entropic effects are more favorable.

The effect of the solvent over the process is shown by the values of the $\mathbf{\Delta\Delta G^{\ddagger}_{solv}}$ in Table 1. This magnitude accounts for the difference between the solvation energies of transition structure and reactants at the gas-phase geometries. In general, solvation increases the barrier except for the case of **FmcdGFmt**. The most unfavorable situations correspond to the two limiting cases **HdG** and **dGOH**, where only the leaving group or the nucleophile is activated. In these cases, the total charge of the system is different from 0 (+1 and −1, respectively), and in the transition structure, this charge is more delocalized that in the reactants. Therefore, the stabilization due to solvation is more important in the reactants than in the transition structure, especially for **dGOH** where the negative charge in the reactants is localized over the OH^- ion. As noted above, the effect of solvation over the barrier in **FmcdGFmt** is favorable. This system also shows a total charge of −1; however, in this case, the nucleobase is not protonated and the heterolytic bond cleavage leads to a transition structure with separated charges in addition to the initial negative charge of the formate anion. Thus, solvent effects are more stabilizing at the transition structure than in the reactant. In all the remaining cases, the total charge of the system is 0 as a result of the positive charge of the activating group and the negative charge of the formate group. In this situation, the charge is more delocalized in the transition structure than in the reactants.

Table 2 Bond orders for N9–C1′ and O···C1′, charge of the sugar ring and C1′–O4′ bond distance (in Å) computed at the TSs

System	Bond order[a]				
	N9–C1′	O···C1′	Total	Q_{dR}	$d_{C1'-O4'}$
HdG	0.057	0.011	0.068	0.824	1.281
dGOH	0.145	0.040	0.185	0.521	1.333
FmcdGFmt	0.031	0.042	0.073	0.738	1.292
HdGFmt	0.103	0.013	0.116	0.695	1.303
ImHdGFmt	0.082	0.014	0.096	0.715	1.298
NHdGFmt	0.041	0.007	0.048	0.804	1.286

[a] Calculated as $n_{ij} = e^{(r_1 - r_{ij})/0.3}$ where r_{ij} is the distance between i and j atoms in the transition structure and r_1 is the distance between i and j in reactants and products (r_1(C–N) = 1.47 Å, r_1(C–O) = 1.43 Å) [48]

In order to get a deeper insight into the associative or dissociative character of the studied transition structures, Table 2 shows the bond order values for N9–C1′ and O_{nucl}···C1′ as well as the charge of the sugar moiety and the C1′–O4′ bond distance. The associative or dissociative character can be related to the sum of bond orders of the new bond formed and the broken one. The mechanism can be defined as associative if this sum is larger in the transition structure than in the reactants and dissociative if the sum is smaller in the transition structure [6]. As mentioned in the introduction, an important aspect related to the nature of the mechanism of the process is the oxacarbenium character of the sugar in the transition structure. It can be observed in Table 2 that the formation of the oxocarbenium is accompanied by the shortening of the C1′–O4′ bond. Actually, the larger the charge of the sugar, the shorter the C1′–O4′ distance is (see Table 2), indicating a double bond formation in the oxocarbenium. In all of the studied cases, the sum of the N9–C1′ and O_{nucl}···C1′ bond orders is much smaller than 1, thus indicating a dissociative character of the mechanism, the smallest values corresponding to **NHdGFmt** and **HdG**. As expected, the two limiting cases considered, where only the leaving group (**HdG**) or the nucleophile (**dGOH**) is activated, show very different values both for the total bond order and for the sugar

charge in agreement with the differences observed in the mechanism (D_N*A_N for **HdG** and A_ND_N for **dGOH**). Particularly interesting is the comparison between **HdG** and **HdGFmt**, which show that the activation of the nucleophile (**HdGFmt**) leads to very different values of the total bond order, the sugar charge and the C1′–O4′ distance, in agreement with the different mechanism observed for both cases and in spite of the similar energy barriers. The values shown in Table 2 for **ImHdGFmt** are similar to those of **HdGFmt** since in this case the nucleobase is also protonated. Overall, results from Table 2 indicate that the oxocarbenium character (Q_{dR}) does not correlate with neither the N9–C1′ nor the $O_{nucl}\cdots$C1′ bond orders, but it follows reasonably well the total bond order, showing that the final transition structure results from the balance between acid–base interactions with dG.

If larger models or whole enzymatic systems were taken into account, other effects different from those studied here would arise. For example, the electric field of the protein could change the stabilization of the ionic species, leading to different protonation states [46]. Furthermore, as we have shown in a previous work [47], protonation of the nucleobase can be influenced by stacking interactions with neighboring aromatic amino acids. However, the present work shows how the strength of an acid and a base modulates the mechanism of the acid–base catalytic hydrolysis of the *N*-glycosydic bond.

4 Conclusions

The catalytic activation of the leaving group and the nucleophile by a general acid or a general base in the hydrolysis of 2′-deoxyguanosine has been investigated by means of density-functional methods. Two limiting cases where only the leaving group is activated, by protonation at the N7 position of the nucleobase, or the nucleophile is a hydroxyl anion, have been investigated and shown to present very similar activation barriers but different mechanisms (D_N*A_N and A_ND_N, respectively). In all the remaining cases, in which both the leaving group and the H_2O nucleophile are simultaneously activated, the reaction mechanism is A_ND_N but with different degrees of dissociative character of the transition structure.

Comparison between the different systems indicates that protonating the nucleobase is essential for the catalysis, since it compensates the negative charge generated at the guanine moiety in the heterolytic cleavage of the *N*-glycosydic bond. When the nucleobase is not protonated, the bond cleavage leads to a situation with charge separation, which is energetically more demanding if the charges are not stabilized by the environment. On the other hand, the comparison between **HdG** and **HdGFmt** shows that the activation of the H_2O nucleophile by formate leads to a less dissociative mechanism but a similar energy barrier. Finally, it is observed that even in similar situations where the interacting acid (imidazolium or methylammonium) leads to guanine protonation, the nature of the hydrogen bonds formed with guanine can also significantly influence the dissociative character of the mechanism. The present work shows how the strength of an acid and a base can modulate the mechanism of the acid–base catalytic hydrolysis of the *N*-glycosydic bond.

Acknowledgments Financial support from the Spanish "Ministerio de Ciencia e Innovación" (MICINN; project CTQ2008-06381/BQU) and the Catalan "Departament d'Innovació, Universitats i Empresa" (DIUE; project 2009SGR-638) and the use of the Catalonia Supercomputer Centre (CESCA) are gratefully acknowledged.

References

1. Loeb LA, Preston BD (1986) Annu Rev Genet 20:201–230
2. Banerjee A, Yang W, Karplus M, Verdine GL (2005) Nature 434:612–618
3. Stivers JT (2008) Chem Eur J 14:786–793
4. Roberts RJ, Cheng XD (1998) Annu Rev Biochem 67:181–198
5. Stivers JT, Jiang YL (2003) Chem Rev 103:2729–2760
6. Berti PJ, McCann JAB (2006) Chem Rev 106:506–555
7. McCullough AK, Dodson ML, Lloyd RS (1999) Annu Rev Biochem 68:255–285
8. O'Brien PJ, Ellenberger T (2003) Biochemistry 42:12418–12429
9. Mazumder D, Bruice TC (2002) J Am Chem Soc 124:14591–14600
10. Mazumder-Shivakumar D, Bruice TC (2005) Biochemistry 44:7805–7817
11. Dinner AR, Blackburn GM, Karplus M (2001) Nature 413:752–755
12. Labahn J, Schärer OD, Long A, Ezaz-Nikpay K, Verdine GL, Ellenberger TE (1996) Cell 86:321–329
13. Lau AY, Schärer OD, Samson L, Verdine GL, Ellenberger T (1998) Cell 95:249–258
14. Bianchet MA, Seiple LA, Jiang YL, Ichikawa Y, Amzel LM, Stivers JT (2003) Biochemistry 42:12455–12460
15. Parikh SS, Walcher G, Jones GD, Slupphaug G, Krokan HE, Blackburn GM, Tainer JA (2000) Proc Natl Acad Sci USA 97:5083–5088
16. Chen X-Y, Berti PJ, Schramm VL (2000) J Am Chem Soc 122:6527–6534
17. McCann JAB, Berti PJ (2007) J Am Chem Soc 129:7055–7064
18. Schramm VL (2003) Acc Chem Res 36:588–596
19. Chen Z-Q, Zhang C-H, Xue Y (2009) J Phys Chem B 113:10409–10420
20. Hunter KC, Millen AL, Wetmore SD (2007) J Phys Chem B 111:1858–1871
21. Ma A, Hu J, Karplus M, Dinner AR (2006) Biochemistry 45:13687–13696
22. Millen AL, Archibald LAB, Hunter KC, Wetmore SD (2007) J Phys Chem B 111:3800–3812
23. Przybylski JL, Wetmore SD (2009) J Phys Chem B 113:6533–6542
24. Millen AL, Wetmore SD (2009) Can J Chem 87:850–863
25. Przybylski JL, Wetmore SD (2010) J Phys Chem B 114:1104–1113

26. Baik M-H, Friesner RA, Lippard SJ (2002) J Am Chem Soc 124:4495–4503
27. Calvaresi M, Bottoni A, Garavelli M (2007) J Phys Chem B 111:6557–6570
28. Cavalieri EL, Vauthier EC, Cossé-Barbi A, Fliszár S (2000) Theor Chem Acc 104:235–239
29. Loverix S, Geerlings P, McNaughton M, Augustyns K, Vandemeulebroucke A, Steyaert J, Versees W (2005) J Biol Chem 280:14799–14802
30. Loverix S, Versees W, Steyaert J, Geerlings P (2006) Int J Quantum Chem 106:565–570
31. Osakabe T, Fujii Y, Hata M, Tsuda M, Neya S, Hoshino T (2004) Chem Bio Inf J 4:73–92
32. Rios-Font R, Bertran J, Rodriguez-Santiago L, Sodupe M (2006) J Phys Chem B 110:5767–5772
33. Rios-Font R, Rodriguez-Santiago L, Bertran J, Sodupe M (2007) J Phys Chem B 111:6071–6077
34. Schyman P, Danielsson J, Pinak M, Laaksonen A (2005) J Phys Chem A 109:1713–1719
35. Shim EJ, Przybylski JL, Wetmore SD (2010) J Phys Chem B 114:2319–2326
36. Becke AD (1988) Phys Rev A 38:3098–3100
37. Lee C, Yang W, Parr RG (1988) Phys Rev B 37:785–789
38. Zhao Y, Truhlar DG (2004) J Phys Chem A 108:6908–6918
39. Becke AD (1993) J Chem Phys 98:1372–1377
40. Raghavachari K, Trucks GW, Pople JA, Head-Gordon M (1989) Chem Phys Lett 157:479–483
41. Frisch MJ, Trucks GW, Schlegel HB, Scuseria GE, Robb MA, Cheesman JR, Montgomery JA, Vreven T, Kudin KN, Burant JC, Millam JM, Iyengar SS, Tomasi J, Barone V, Mennucci B, Cossi M, Scalmanu G, Rega N, Petersson GA, Nakatsuji H, Hada M, Ehara M, Toyota K, Fukuda R, Hasegawa J, Ishida M, Nakajima T, Honda Y, Kitao O, Nakai H, Klene M, Li X, Knox JE, Hratchian HP, Cross JB, Adamo C, Jaramillo J, Gomperts R, Stratmann RE, Yazyev O, Austin AJ, Cammi R, Pomelli C, Ochterski JW, Ayala PY, Morokuma K, Voth GA, Salvador P, Dannenberg JJ, Zakrzewski VG, Dapprich S, Daniels AD, Strain MC, Farkas O, Malick DK, Rabuck AD, Raghavachari K, Foresman JB, Ortiz JV, Cui Q, Baboul AG, Clifford S, Cioslowski J, Stefanov BB, Liu G, Liashenko A, Piskorz P, Komaromi I, Martin RL, Fox DJ, Keith T, Al-Laham MA, Peng CY, Nanayakkara A, Challacombe M, Gill PMW, Johnson B, Chen W, Wong MW, Gonzalez C, Pople JA (2004) Gaussian 03. Gaussian Inc., Wallingford
42. McQuarrie D (1986) Statistical mechanics. Harper and Row, New York
43. Cossi M, Rega N, Scalmani G, Barone V (2003) J Comput Chem 24:669–681
44. Reed AE, Curtiss LA, Weinhold F (1988) Chem Rev 88:899–926
45. Weinhold F, Carpenter JE (1988) The structure of small molecules and ions. Plenum, New York
46. Kamerlin SCL, Haranczyk M, Warshel A (2008) J Phys Chem B 113:1253–1272
47. Noguera M, Rios-Font R, Rodriguez-Santiago L, Solans-Monfort X, Oliva A, Bertran J, Sodupe M (2009) Theor Chem Acc 123:105–111
48. Pauling L (1947) J Am Chem Soc 69:542–553